Nigerian Journal of Environmental Sciences and Technology (NIJEST)
www.nijest.com
ISSN (Print): 2734-259X | ISSN (electronic): 2734-2603
Vol 7, No. 2 July 2023, pp 337 - 346

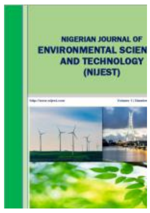

Application of Stability Estimator Model in the Determination and Adjustment of Deformation Monitoring Points of Jimeta Bridge

Damuya, S. T[1]., Takana, A.[2]*. and Edan, J. D.[3]

[1,2&3]Department of Surveying and Geoinformatics Modibbo Adama University, Yola

Corresponding Author: *takana.abubakar@gmail.com

https://doi.org/10.36263/nijest.2023.02.0424

ABSTRACT

Establishment of stable deformation monitoring points is a vital step in the monitoring of the stability of deformable structures. This research dwells on the establishment of a network of points to monitor the stability of Jimeta Bridge. Approximate horizontal coordinates of the monitoring points were first obtained using the GNSS receiver. The vertical coordinates of the same points were observed using a precise levelling operation. The horizontal and vertical coordinates of the monitoring points were adjusted to get a stable network of points for the monitoring of the bridge. The adjustment was achieved using a Stability estimator model which is designed based on the principle of free network. The results show that the 66th baseline configuration returned the maximum redundancy number of the reliability matrix of 0.59880000000000 and a minimal trace of 0.00539266393068631. The aposteriori variances were computed and found to be 0.4465, for the test on reference points and 0.6177 for the test on object points. The computed aposteriori variance both falls between the lower and the upper limit. This signifies that the geometry of the monitoring network points remains intact with no distortion. The network of the monitoring points is therefore safe to be utilised in the monitoring of the stability of the Jimeta Bridge.

Keywords: Deformation Monitoring, Mathematical Model, Least Squares Adjustment, Stability Estimator and Engineering Structure

1.0. Introduction

Deformation monitoring is an important tool used by engineers to keep track of the behaviour of structures with time. It provides quantitative and reliable information in the study of the stability of natural and man-made features in the environment, for risk assessment and for the timely adoption of appropriate measures (Sylvester *et al.*, 2018; Wieser and Coper 2017; Kumar, *et al.*, 2021). Deformation analysis can improve the understanding of the deformation characteristics of structures and can facilitate improvements to engineering designs. Deformation analysis is required for the safe operation of structures such as dams, bridges, viaducts, earthworks, high-rise buildings, and light rail transit stations (Massamba *et al.*, 2019).

Measurements and the analysis of deformations of structures constitute a special branch of geodesy. The methods used for the measurement of deformation are generally classified into surveying (geodetic) and non-surveying (geotechnical) methods. The surveying techniques include conventional, photogrammetric, satellite and remote sensing. Non-surveying techniques such as geotechnical measurement, using laser, tilt meters, strain meters, extensor meters, joint meters, plumb lines, micrometres, etc. Each main measurement technique has its advantages and drawbacks. Surveying techniques, through a network of points interconnected by angle and distance measurement, usually supply sufficient redundant observations for statistical evaluation of their quality and detection of errors. The surveying techniques give global information on the behaviour of deformable structures, while the non-surveying techniques give localized and locally disturbed information without any check unless compared with some other independent measurements (Ono *et al.*, 2018).

Surveying techniques have traditionally been used mainly for determining the absolute displacement of selected points on the surface of the object concerning some stable reference points. The techniques require long-time monitoring of the structure's movement typically taking observation to monitoring points on the structure from external reference points. These external reference points are established on the stable ground away from the structure. In surveying techniques of deformation studies, the information on the absolute movements of object points concerning some stable reference points is crucial. Network points (reference and object ones) need to be stable (undisplaced) during the deformation monitoring (Duchnowski and Wyszkowska, 2022). Any unstable reference points must be identified before embarking on deformation monitoring of structures, otherwise, the calculated displacements of object points and subsequent analysis and interpretation of the deformation of the structure may be distorted (Alademomi *et al.,*2020)

This research focuses on the establishment of such stable monitoring network points around the Jimeta Bridge to have a reliable base for a monitoring scheme of the bridge. This is important because bridges of such magnitude are usually confronted with truck overloading which causes fatigue on the bridge components and subsequently shortens the service life of bridges (Wardhana and Hadipriono 2003; Biezma and Schanack, 2007). In some extreme cases, the weight of the overloaded trucks may exceed the load-carrying capacity of the bridge and directly cause bridge collapse. The deterioration mechanism is influenced by various factors including material properties, environmental conditions, and live load situation (Kim *et al.,* 2013). The risk of bridge deterioration cannot be eliminated, however, a good maintenance program including regular inspection and proper rehabilitation will slow down this process (Biezma and Schanack, 2007). Fires on bridges are commonly caused by collisions or other accidents (Bai, *et al.*, 2006). Increase of temperature (in the range of 800-900^{0}C) within the first few minutes of five initiations and the temperature can rise to 1,000^{0}C or higher in the first 30 minutes. The rapid temperature rise can create large thermal gradients in the structural members and consequently cause spalling of the concrete and local buckling of steel members (Peng, *et al.*, 2008). Moreover, fires can lead to a significant decrease in the load-carrying capacity of the structural members due to a reduction in the strength and stiffness of materials, which can further lead to partial or full collapse of bridges (Bai, *et al.,* 2006). Jimeta Bridge and other gigantic engineering structures alike are subject to deformation as such there is a need to have in place a system for monitoring the structures to give adequate information on their stability.

Before the commencement of a reliable and sustainable structural monitoring process, a network of monitoring points needs to be established. The success of the monitoring scheme depends largely on the reliability of the monitoring network points (Samuel *et al.,* 2021). This research focuses on the establishment of a network of monitoring points to serve as a base for the monitoring of Jimeta Bridge. The network is designed in such a way that the monitoring system will achieve the prescribed monitoring accuracy of points and can be sensitive to statistical tests for the detection of outliers in measurement and also to resist undetected gross errors.

2.0. Methodology

2.1 The Study Area

Jimeta Bridge is located in Yola, the capital city of Adamawa state. It is a strategic civil engineering structure lying across the River Benue trough. The bridge is a major link connecting the north-central part and south-central parts of the state. River Benue serves as a natural boundary between Girei local government and Yola north local government area. The bridge lies between latitude 9° 12’ and 30.20” N and between longitude 12° 28’ and 53.26” E of the Greenwich meridian with a total length of 1.422 Km as shown in Figure 1.

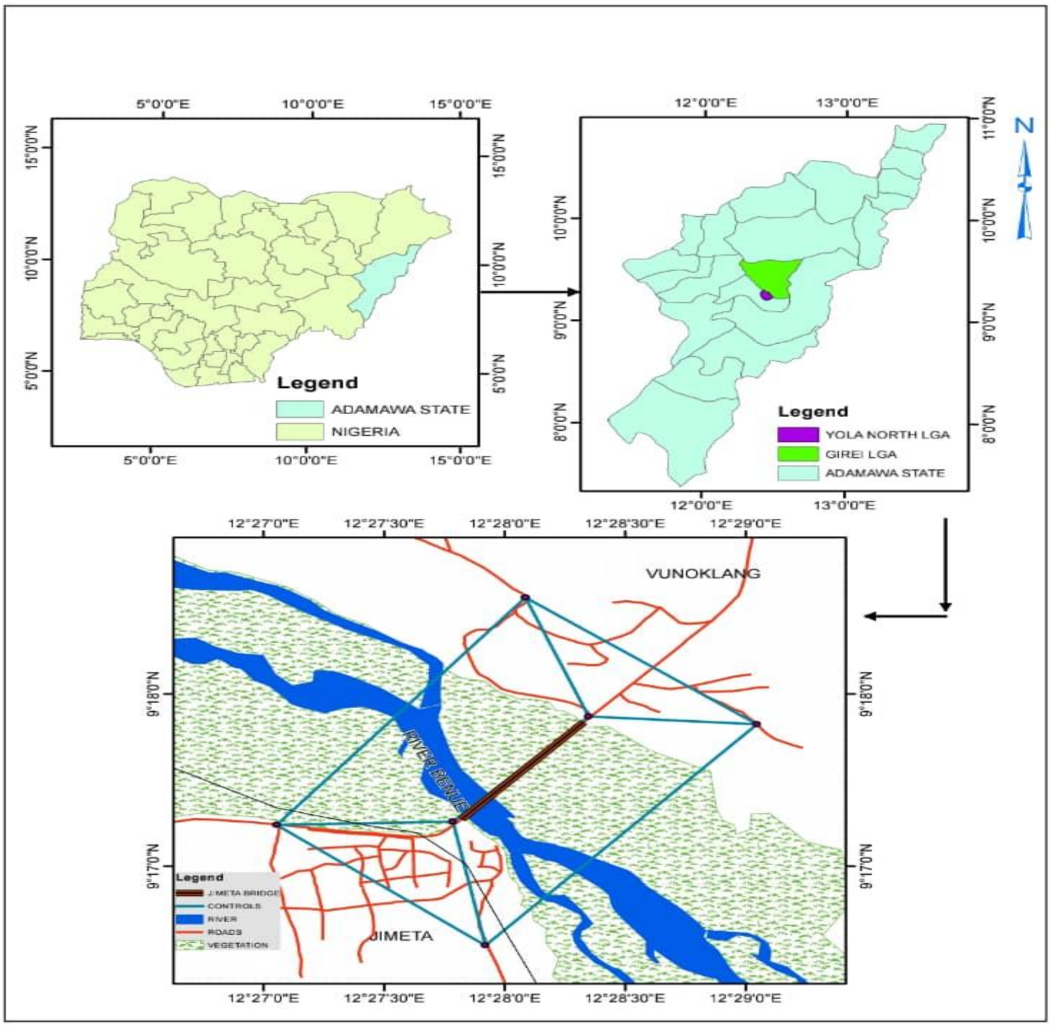

Figure 1: Jimeta Bridge

2.2 Materials

The materials used in this research include A Hi-target Differential GNSS receiver and Leica NA2 with its accessories. The GNSS receiver was used in the observation of the approximate horizontal coordinate of the monitoring station. The Leica NA2 was used in the determination of height components of the monitoring points.

2.2 Method

The methodology adopted was the Homogenous and Isotropic Optimization procedures, followed by a check on the reliability of the optimization of the points and then the post-processing and the adjustment of the horizontal and vertical coordinates of the points.

2.2.1 Determination of Optimal Locations of Monitoring Points

As a prelude to optimal locations of points for deformation monitoring, approximate coordinates of the points were obtained using a GNSS receiver. During the field reconnaissance operations, points were selected bearing the following in mind;

(1) As much as possible the proposed stations should be kept away from reflective objects/surfaces to avoid multipath effects.

(2) The station was placed on firm and stable ground and not on soil susceptible to erosion.

(3) On good sky visibility with a mask angle of approximately 8^0 to 15^0 free of obstruction.

(4) The ground network stations were selected on the locations that ensure a square-shaped network.

2.2.2 Homogenous and Isotropic Optimization

In the optimization, a design matrix of partial derivatives and a weight matrix of the covariance derived from baseline composition were developed. The design matrix was formed based on the baseline configuration observed in the network with the non-zero elements of the design matrix as either 1 or -1 indicating the configuration of network points. A weight matrix was formed based on the three observed baseline components which are correlated. A covariance matrix of dimensions 3x3 was derived for each baseline as a product of the least square adjustment of the carrier-phase measurements.

To replicate the covariance block diagonal matrix for the entire baseline in the network, an adjustment program package by Glilani 2006 was adopted.

Using the approximate coordinates obtained in Table 1 below, the network points were adjusted

Table 1: Approximate Coordinates of JBMP

Id	Latitude	Longitude	Height.	Remarks
JBMP1	12°27'47.13686" N	9°17'15.45652" E	585.908	Reference Point
JBMP2	12°28'21.00943" N	9°17'52.19077" E	586.709	Reference Point
JBMP3	12°28'05.24808" N	9°18'33.59349" E	622.147	Reference Point
JBMP4	12°29'02.93475" N	9°17'49.41469" E	585.751	Reference Point
JBMP5	12°27'55.24270" N	9°16'32.36938" E	616.735	Reference Point
JBMP6	12°27'03.20425" N	9°17'14.31594" E	580.488	Reference Point
MP7	12°27'51.37233" N	9°17'18.30360" E	592.391	Object Point
MP8	12°28'00.08442" N	9°17'28.02376" E	597.599	Object Point
MP9	12°28'08.80778" N	9°17'37.74979" E	592.860	Object Point
MP10	12°28'17.53251" N	9°17'47.48110" E	587.988	Object Point
MP11	12°28'12.78007" N	9°17'42.94371" E	590.299	Object Point
MP12	12°28'04.06212" N	9°17'33.21774" E	595.009	Object Point
MP13	12°27'55.36819" N	9°17'23.50157" E	597.979	Object Point

to plan for the best geometry of the survey. The aposteriori covariance matrix of the parameters of the network was determined using the mathematical model developed in Equation 1 below.

$$Q_{xx} = (A^T PA + DD^T)^{-1} \quad (1)$$

Where:

Q_{XX} is the cofactor matrix, A is the design matrix, P is the weight matrix, and D is the datum matrix

To optimize the locations of the network points the initial geometry of the approximate coordinates were varied away from the center of each station that makes up the monitoring network. At each initial network station, 4 quadrants were created and each quadrant was further subdivided into 2, thereby bringing the number of subdivisions at each station to 8 equals. Within each subdivision, 10 points were selected at random hence 80 potential monitoring points for the Jimeta bridge network were designed. Among these 80 potential networks, the mathematical model returned only one desired result (minimum trace and maximum reliability) as the optimal network for the deformation monitoring network of Jimeta Bridge.

During the optimization process above, the objective function (minimum trace and maximum reliability) was achieved iteratively starting from the initial approximate coordinate as the first observation plan to the last observation plan. The known parameters in the optimization were the weight of the observation (P), the design matrix of observation (A) and the datum matrix (D), while the unknown parameters are the cofactor matrix (Q_{xx}) from the first to the last observation plan. After the cofactor matrix had been computed, the Eigenvalue from the first to the last observation plan was extracted from the diagonal elements of the cofactor matrix. The square root of the Eigenvalues is the error ellipses and sum of the Eigenvalues and the trace of the cofactor matrix (Q_{xx}) of each observation plan in the network. Minimum error ellipses of a network signify a homogenous network while a minimum trace of cofactor signifies an isotropic network.

2.2.3 Reliability Optimization of Monitoring Points

To have a well-designed network with high reliability is the focus of this research. To achieve this network the following criteria by Ghilani and Wolf (2006) were adopted:

(1) Network with sufficient geometric checks to allow observational blunders to be detected and removed.
(2) The redundancy number of individual observations should approach their maximum value of 1 to minimize the size of the undetected blunders in a network.
(3) Redundancy numbers above 0.5 are generally sufficient to provide well-checked observations.

To meet the above condition, equation 2 adopted from the work of Kuang (1996) was applied to determine the redundancy number.

$$R = I_n - A(A^T PA + DD^T)^{-1} A^T P \qquad (2)$$

Where,

I_n is an identity matrix with *n* observations, and the other parameters are the same as introduced in Equation 1.

2.2.4 Field Measurements and Data Processing

A Hi-target Differential GNSS receiver was used in the observation of horizontal coordinates of the reference frame and object points. This was necessitated due to its advantage of spanning large distances with good precision. The measurement was carried out on all the points with a station occupation period of one hour**.** After the field measurements, the data was post-processed using GNSS solution software version 3.7. A precise levelling operation using Leica NA2 was carried out to determine the height components of the monitoring stations. The use of levelling operation was chosen to avoid errors due to mask angle, height of antenna, ionospheric, stratospheric, tropospheric, and multipath delays among others that are inherent in GNSS receivers (Adeleke 2022). The height levelling height was connected to a Federal Benchmark (FBM 1) located in the premises of the Adamawa State Local Government Service Commission. The levelling observation was reduced and checked. The levelling data was later adjusted using the least squares adjustment model.

For the levelling network, the weight of each observation is inversely proportional to the distance in kilometres of the level run or loop distances. The sets of observation equation models 3 to 6 below were adopted for the least square adjustment.

$$L^0 = f(X^0) \qquad (3)$$

$$X^a = X^0 + x \qquad (4)$$

Form a set of normal equations and compute correction/solution vector (x)

$$x = -(A^T PA)A^T PL \qquad (5)$$

Compute adjusted parameters

$$X^a = X^0 + x \qquad (6)$$

Compute the standard error of adjusted parameters

Aposteriori $\left(\widehat{\delta_0^2}\right) = V^T PV / n - m \qquad (7)$

Where

X^0 is the approximate parameters, X^a is the adjusted parameters, x is the corrections vector, L^0 is the adjusted observation, L is the elements of observation, V is the residual vectors, n is the number of equations, and m is the number of parameters. The other parameters are as described above.

2.2.5 Blunders detection in GPS observation

To improve GNSS observation in this network, a series of procedures were followed to analyze the data for internal consistency and to eliminate possible blunders. Analysis of Loop Closure: In Figure 2, the points JBMP01-JBMP06 are called points A-F for brevity in explaining loop closure. As such, a closed loop was formed by points FAEDBCF, AEDBA and FABCF in the first and second epoch measurements.

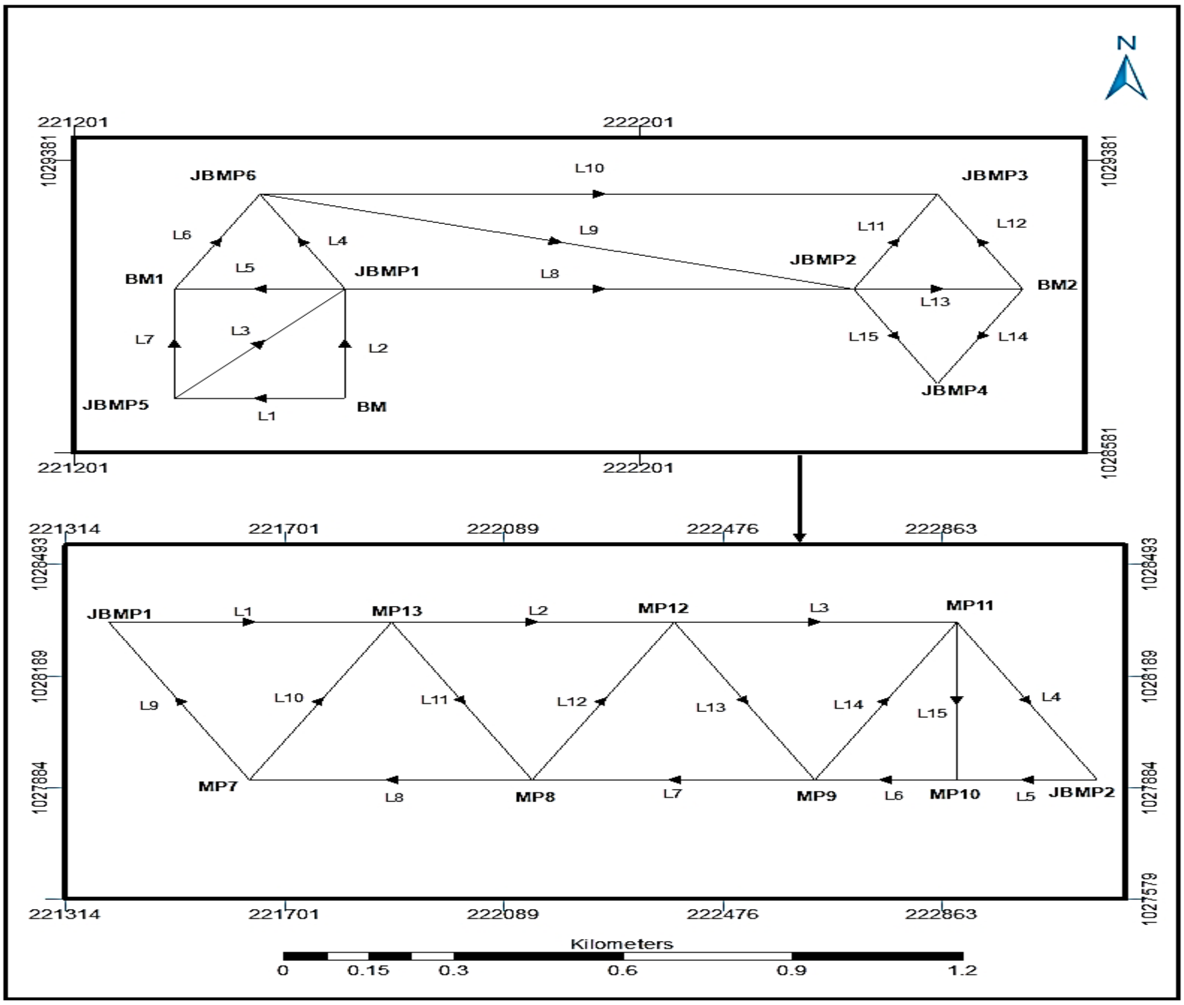

Figure 2: Arrangement of Jimeta Bridge Monitoring Points

In a closed loop, the summation of the ΔX components should equal zero. The same condition applies to ΔY and ΔZ components.

Loop closure for FAEDBCF

$$\begin{bmatrix} \Delta X_{FA}, \Delta X_{AE}, \Delta X_{ED}, \Delta X_{BD}, \Delta X_{BC}, \Delta X_{CF} \\ \Delta Y_{FA}, \Delta Y_{AE}, \Delta Y_{ED}, \Delta Y_{BD}, \Delta Y_{BC}, \Delta Y_{CF} \\ \Delta Z_{FA}, \Delta Z_{AE}, \Delta Z_{ED}, \Delta Z_{BD}, \Delta Z_{BC}, \Delta Z_{CF} \end{bmatrix} = \begin{bmatrix} C_X \\ C_Y \\ C_Z \end{bmatrix}$$

$$\begin{bmatrix} -288.49,\ 186.32,\ -849.09,\ 262.23,\ -64.92,\ 753.95 \\ -12.27,\ -1288.00,\ 2218.65,\ 127.88,\ 1256.32,\ -2302.58 \\ 1319.28,\ 249.84,\ 2024.32,\ -1257.71,\ -465.31,\ -1870.42 \end{bmatrix} = \begin{bmatrix} 0 \\ 0 \\ 0 \end{bmatrix}$$

Loop closure for AEDBA

$$\begin{bmatrix} \Delta X_{AE}, \Delta X_{ED}, \Delta X_{DB}, \Delta X_{BA} \\ \Delta Y_{AE}, \Delta Y_{ED}, \Delta Y_{DB}, \Delta Y_{BA} \\ \Delta Z_{FA}, \Delta Z_{ED}, \Delta Z_{DB}, \Delta Z_{BA} \end{bmatrix} = \begin{bmatrix} C_X \\ C_Y \\ C_Z \end{bmatrix}$$

$$\begin{bmatrix} 186.32, -849.09, \ 262.23, \ 400.54 \\ -1288.00, 2218.65, 127.88, -1058.53 \\ 249.84, \ 2024.32, -1257.71, -1016.45 \end{bmatrix} = \begin{bmatrix} 0 \\ 0 \\ 0 \end{bmatrix}$$

Loop closure for FABCF

$$\begin{bmatrix} \Delta X_{FA}, \Delta X_{AB}, \Delta X_{BC}, \Delta X_{CF} \\ \Delta Y_{FA}, \Delta Y_{AB}, \Delta Y_{BC}, \Delta Y_{CF} \\ \Delta Z_{FA}, \Delta Z_{AB}, \Delta Z_{BC}, \Delta Z_{CF} \end{bmatrix} = \begin{bmatrix} C_X \\ C_Y \\ C_Z \end{bmatrix}$$

$$\begin{bmatrix} -288.49, \ 400.54, -64.92, 753.95 \\ -12.27, \ 1058.53, \ 1256.32, -2302.58 \\ 1319.29, \ 1016.45, -465.31, -1870.42 \end{bmatrix} = \begin{bmatrix} 0 \\ 0 \\ 0 \end{bmatrix}$$

3.0 Results and Discussion

Table 2 shows the reliability of observational plans for JBMP. Column one in Table 2, is the serial numbers of the observed baseline, column two is the observed baseline and column three is the mean of redundancy numbers (observational reliability) in each observational plan cofactor matrix. Among the 80 potential locations of the monitoring points, the 66th baseline configuration returned the maximum redundancy number of the reliability matrix of 0.59880000000000 and a minimal trace of 0.00539266393068631 as shown in Tables 2 and 3 respectively. Furthermore, the aposteriori variances were computed and found to be 0.4465, which falls within the range of lower limit 0.2414 and upper limit 2.2875 for the test on reference points and 0.6177 which falls within the range of lower limit 0.2725 and upper limit 2.1918 for test on object points.

Table 2: Reliability Matrix of Observational Plan

S/N	Observed Baseline	Extracted Mean of Diagonal Elements of Network design Reliability Matrix(R_N)
1	1-1	0.599873244444445
2	1-2	0.599875511111111
3	1-3	0.599873200000000
4	1-4	0.599873244444445
5	1-5	0.599875511111111
6	1-6	0.599875511111111
7	1-7	0.599875511111111
8	1-8	0.599875511111111
9	1-9	0.599875511111111
‘	,	,
67	7-6	0.59880000000000
‘	‘	,
,	,	,
71	8-1	0.599873200000000
72	8-2	0.599873244444445
73	8-3	0.599873244444444
74	8-4	0.599873200000000
75	8-5	0.599873244444444
76	8-6	0.599873155555556

77	8-7	0.599873111111111
78	8-8	0.599873111111111
79	8-9	0.599873155555556
80	8-10	0.599873155555556

Table 3 is the trace of observational plans for JBMP. Column one is the serial number of the observed baseline, column wo in Table 3 is the observed baseline and Column three is the trace (sum of the diagonal elements) of each observational plan cofactor matrix. This result has shown that the 66th observational plan is a homogeneous, isotropic and reliable network that gave the best observational quantities as shown in Table 3.

Table 3: Trace of Observational Plan

S/N	Observed Baseline	Extracted Trace of Cofactor Matrix (Q_{XX})
1	1-1	0.00569544853705775
2	1-2	0.00559376768184589
3	1-3	0.00569744871506059
4	1-4	0.00569544593539938
5	1-5	0.00559375878953612
6	1-6	0.00559376354353315
7	1-7	0.00559376020811612
8	1-8	0.00559376020811612
9	1-9	0.00559375878953612
‘	‘	‘
67	7-6	0.00539266393068631
‘	‘	‘
‘	‘	‘
71	8-1	0.00569743747643746
72	8-2	0.00569543800854719
73	8-3	0.00569544846209222
74	8-4	0.00569743748039433
75	8-5	0.00569544846209222
76	8-6	0.00569944585712106
77	8-7	0.00570144455065002
78	8-8	0.00570144125210921
79	8-9	0.00569944247397929
80	8-10	0.00569944247397929

Table 4 shows the GPS post-processed results of the monitoring points. Column one is the numbers of the initial monitoring points, and columns two and three are the geographic coordinates of the monitoring points that is the latitude and longitude respectively. Column four is the height component of the monitoring points obtained via levelling while column five is the remarks.

Table 4: GPS Post-processed horizontal Coordinates and heights of monitoring points

ID	**Latitude**	**Longitude**	**Heights**	**Remarks**
JBMP1	12°27'47.13686" N	9°17'15.45652" E	585.908	Reference Point
JBMP2	12°28'21.00943" N	9°17'52.19077" E	586.709	Reference Point
JBMP3	12°28'05.24808" N	9°18'33.59349" E	622.147	Reference Point
JBMP4	12°29'02.93475" N	9°17'49.41469" E	585.751	Reference Point
JBMP5	12°27'55.24270" N	9°16'32.36938" E	616.735	Reference Point
JBMP6	12°27'03.20425" N	9°17'14.31594" E	580.488	Reference Point
MP7	12°27'51.37233" N	9°17'18.30360" E	592.403	Object Point
MP8	12°28'00.08442" N	9°17'28.02376" E	597.618	Object Point
MP9	12°28'08.80778" N	9°17'37.74979" E	592.869	Object Point
MP10	12°28'17.53251" N	9°17'47.48110" E	588.014	Object Point
MP 11	12°28'12.78007" N	9°17'42.94371" E	590.316	Object Point
MP 12	12°28'04.06212" N	9°17'33.21774" E	595.026	Object Point
MP 13	12°27'55.36819" N	9°17'23.50157" E	597.984	Object Point

4.0 Conclusion

This study focused on the determination and adjustment of deformation monitoring points. The monitoring points consists of reference points and object points which together form a network of monitoring scheme. The monitoring points were selected to get the optimum location of the point for a good monitoring scheme. The coordinates of the points were adjusted and the results of the adjustment have shown that among the 80 potential locations of the monitoring points, the 66th baseline configuration returned the minimal trace of 0.00539266393068631and a maximum redundancy number of the reliability matrix as 0.599880000000000. This shows that the 66th observational plan has a homogeneous, isotropic and reliable network that gave the best observational quantities. In addition, the aposteriori variances were found to be 0.4465 which falls within the range of lower limit 0.2414 and upper limit 2.2875 for the test on reference points and 0.6177 which falls within the range of lower limit 0.2725 and upper limit 2.1918 for test on object points. This signified that no gross errors such as gross measurement errors, booking errors, mistakes in identification of points, unstable monuments, or centering errors, exist in the observations. The result further proves that the geometry of the monitoring network remains intact without distortion as the shape of the monitoring network in the design stage. The points can therefore be used for the monitoring of the Jimeta Bridge.

References

Alademomi A.S, Mayaki A.O, Daramola O.E, Salami T.J and Olaleye J.B (2020): Establishment of Deformation and Subsidence Monitoring Baseline in the Coastal Environment: A Case Study of University of Lagos. *South African Journal of Geomatics*, Vol. 9. No. 1 pp 13-30

Adeleke, Olusayo (2022). Determination of Optimal Antenna Height and Mask Angle of Global Positioning System (GPS) Receiver for Point Positioning. *African Journal on Land Policy and Geospatial Sciences*, [S.l.], v. 5, n. 4, p. 696-706, ISSN 2657-2664.

Bai, Y., Burkett, W.R., and Nash, P.T. (2006). Rapid Bridge Replacement Under Emergency: A case study. *Journal of Bridges Engineering* 11 (3): 266- 373

Baselga S. (2011). Second Order Design of Geodetic Networks by the Simulated Annealing Method. *Journal of Surveying Engineering*. 137(4):167-173. Doi:10.10201/(ASCE)SU:1943-5428.0000053

Biezma, M.V., and Schanack, F. (2007). Collapse of steel bridges. *Journal of performance of constructed facilities* 21(5): 398-405.

Duchnowski, R., & Wyszkowska, P. (2022). Unstable Object Points during Measurements. Deformation Analysis Based on Pseudo Epoch Approach. *Sensors (Basel, Switzerland)*, *22*(23). https://doi.org/10.3390/s22239030

Ghilani, C. D. and Wolf, P.R. (2006). Adjustment Computation: Spatial Data Analysis, Fourth Edition, John Wiley and Sons, Inc. ISBN. 978-0-471-69728-2.

Kim, S., Frangopol, D.M., and Soliman, M. (2013). A Generalized Probabilistic Framework for Optimum Inspection and Maintenance Planning. *Journal of Structural Engineering* 139 (3):435- 447

Kuang, S. (1996). Geodetic Network Analysis and Optical Design: Concept and Applications, Ann Arbor press Inc., Chelsea, Michigan.

Kumar, P., Debele, S. E., Sahani, J., Rawat, N., Marti-Cardona, B., Alfieri, S. M., Basu, B., Basu, A. S., Bowyer, P., Charizopoulos, N., Jaakko, J., Loupis, M., Menenti, M., Mickovski, S. B., Pfeiffer, J., Pilla, F., Pröll, J., Pulvirenti, B., Rutzinger, M., Zieher, T. (2021). An verview of monitoring methods for assessing the performance of nature-based solutions against natural hazards. *Earth-Science Reviews*, *217*, 103603. https://doi.org/10.1016/j.earscirev.2021.103603

Massamba Fall, Zhengguo Gao, Becaye Cissokho Ndiaye (2019). Subway tunnels. Displacement analysis due to two different communication channel construction procedures. *Heliyon*.https://doi.org/10.1016/heliyon 2019.e01949.Vol. 5 issue 6

Ono, M. N., Eteje, S. O., Aghedo, H. O. and Oduyebo, F. O. (2018). Monitoring and analysis of Deformation of Ikpoba River bridge, Benin City, Edo State, Using Global Positioning System. *Nigerian Journal of Geodesy (NJG)*, Vol. 2, No. 1, pp 93-108

Peng, G.F., Bian, S.H., Guo, Z.Q., Zhao, J., Peng, X.L., and Jiang, Y.C. (2008). Effect of Thermal Shock Due to Rapid Cooling on Residual Mechanical Properties of Fibre Concrete Exposed to High Temperatures. *Construction of Building materials* 22 (5): 948-955

Samuel O. A., Hamed O. O., Hannah O. A,. Chukwuma J. O., Samuel A. A. and Usman O. A (2021). Establishment of a Geodetic Network for Deformation Monitoring of the Third Mainland Bridge, Lagos, Nigeria. *Third Intercontinental Geoinformation day (IGD) Mesin Turkey*

Sylvester Okiemute, Eteje Ono, M.N. and Olujimi, Oduyebo. (2018). Monitoring and Analysis of Vertical and Horizontal Deformations of a Large Structure Using Conventional Geodetic Techniques. 8. 52-61. 10.5281/zenodo.2529964. *Journal of Environment and Earth Science* www.iiste.org ISSN 2224-3216 (Paper) ISSN 2225-0948 (Online) Vol.8, No.12

Wadhana K. and Hadipriono F.C. (2003). Analysis of Recent Bridge Failures in the United States. *Journal of Performance of Constructed Facilities*, 17. 144-150 https://doi.org//10.061/(ASCE)0887-3828(2003)17:3(144)

Wieser, A. and Capra A. (2017). Special Issue: Deformation Monitoring. *Applied Geomatics*, Vol. 9, No. 2, pp 79- 80. doi.org/10.1007/s12518-017-0192-0.

Cite this article as:

Damuya, S. T., Takana, A. and Edan, J. D., 2023. Application of Stability Estimator Model in the Determination and Adjustment of Deformation Monitoring Points of Jimeta Bridge. *Nigerian Journal of Environmental Sciences and Technology*, 7(2), pp. 337-346. https://doi.org/10.36263/nijest.2023.02.0424.